Düzce University Journal of Science & Technology

Research Article

Preparation of a Clay Composite Containing Poly(*o*-toluidine) and Halloysite, and Examining of Its Performance as a Humidity Sensor

Meryem KALKAN ERDOĞAN [a], Meral KARAKIŞLA[a,*]

[a] *Department of Chemistry, Faculty of Science, Ankara University, Ankara, TURKEY*
** Corresponding author's e-mail address: meral.karakisla@gmail.com*
DOI: 10.29130/dubited.836431

ABSTRACT

This study outlines the production of an electrically conductive clay-based composite containing the halloysite as clay mineral and poly(*o*-toluidine) (POT) as a conductive filler. In the study, conductive POT/halloysite composite was obtained by in situ oxidative polymerization of *o*-toluidine using ammonium persulphate (APS) as an oxidant between the halloysite layers. By changing the polymerization conditions such as polymerization time, *o*-toluidine concentration, APS, and the concentration of HCl solution used as the reaction medium, the composite with the highest conductivity (7.5×10^{-5} S.cm^{-1}) was obtained. Structural and morphological changes and thermal behaviors that occurred after the composite formation was revealed using various characterization techniques such as FTIR, XRD, TGA, and SEM. The usability of the prepared POT/halloysite composite as humidity sensing material was tested in comparison with the pure POT component of the composite at a relative humidity (% RH) varied between 41-94 (%). Accordingly, it was found that the composite exhibited a fairly regular resistance change to varying relative humidity compared to pure POT polymer.

Keywords: *conductive clay-composite, poly(o-toluidine), halloysite, humidity sensing*

Poli (o-toluidin) ve Halloysit İçeren Bir Kil Kompozitinin Hazırlanması ve Nem Sensörü Olarak Performansının İncelenmesi

ÖZET

Bu çalışma, kil minerali olarak halloysit ve iletken bir dolgu maddesi olarak poli (o-toluidin) (POT) içeren elektriksel olarak iletken kil bazlı bir kompozitin üretimini özetlemektedir. Çalışmada, iletken POT / halloysit kompoziti, o-toluidinin, halloysit tabakaları arasında oksidant olarak amonyum persülfat (APS) kullanılarak in-situ oksidatif polimerizasyon yöntemi ile elde edildi. Polimerizasyon süresi, o-toluidin derişimi, APS ve reaksiyon ortamı olarak kullanılan HCl çözeltisi derişimi gibi polimerizasyon koşulları değiştirilerek en yüksek iletkenliğe sahip kompozit (7.5×10^{-5} Scm^{-1}) elde edildi. Kompozit oluşumundan sonra meydana gelen yapısal ve morfolojik değişiklikler ve termal davranışlar FTIR, XRD, TGA ve SEM gibi çeşitli karakterizasyon teknikleri kullanılarak ortaya konuldu. Hazırlanan POT / halloysit kompozitin nem algılama malzemesi olarak kullanılabilirliği, 41-94 arasında değişen bir bağıl nemde (% RH) kompozitin saf POT bileşeni ile karşılaştırılarak test edilmiştir. Buna göre kompozitin, saf POT polimere kıyasla değişen bağıl neme karşı oldukça düzenli bir direnç değişikliği sergilediği bulundu.

Keywords: *iletken kil kompozit, poli(o-toluidin), halloysit, nem sensörü*

Received: 05/12/2020, Revised: 23/01/2021, Accepted: 28/01/2021

I. INTRODUCTION

Due to possessing excellent chemical and physical properties of its components, the electrically-conductive clay composites that are fabricated by the combination of conjugated conductive polymers with the clay minerals have participated in different application fields, such as humidity and temperature sensing [1-3], drug delivery [4], biosensor material development [5], anticorrosion application[6], electrode modification [7], filling agent for the conductivity applications [8], supercapacitor fabrication [9]and electrochemistry [10, 11]. For that reason, many attempts have been made for the fabrication of conductive clay-based composites using different chemical and electrochemical methods [5, 12, 13]. Among them, thanks to enabling one-step and facile modification of clay minerals with the conjugated polymers through coating or intercalation, the in-situ oxidative polymerization can be found promising by the researchers. In that method, the aqueous or non-aqueous dispersion of clay minerals can be simultaneously modified by the conductive polymers, using an oxidizing agent for the polymerization of a conjugated monomer, densely and homogeneously. Using this method, different conductive clay composites containing different conductive polymers, such as polyaniline and its derivatives/copolymers, polypyrrole, and polythiophene have been prepared in the literature [2-4, 14-17]. In this study, we preferred the synthesis of one of the most conductive polyaniline derivatives, POT, as the conductive polymer component of the composite by in-situ oxidative polymerization.

The matrix of the composite, halloysite, is a super-fine clay of kaolin group, with a formula of 1:1 layer of $Al_2Si_2O_5(OH)_4.2H_2O$, and has a hollow tubular structure with multi layers [18]. Due to its versatile properties, such as high surface area, high hydrophilicity, tunable structure by the chemical modification, economic tubular raw material compared to its alternatives, it has been an attractive material to employ in various researches [13, 19]. Although there have been a lot of studies regarding the conductive polymer/halloysite composites in the form of nanotubular structure [6, 9, 12, 13, 20-27], to our knowledge, no study has been published for the fabrication of POT/halloysite composite in the literature. Most of these articles contain only the preparation of polyaniline/halloysite composites without investigating the imparted properties of the components. A few reports have issued the application of developed-composite as supercapacitors, adsorption, and gas separation [21, 25-27].

Different from these reports, in this work, we aimed to fabricate a conductive POT/halloysite composite for revealing its potential in the use of humidity sensing between 41%-94 % RH range. For that purpose, we focused on the preparation of relatively the highest electrically conductive composite, by alteration the experimental conditions in detail. We also investigated the imparted characteristics of the components by different techniques.

II. MATERIALS&METHODS

A. MATERIALS

Halloysite (Esan, Eczacıbaşı Industrial Raw Materials Company, Turkey) was used in the experiments after subjecting to a drying process in the vacuum oven at 75 °C for 24 hours. *o*-toluidine (98%) (Aldrich, Turkey) was distilled under reduced pressure (8 mmHg/60^{o}C) before using in the polymerization. The other chemicals that are presented in the appearance order of the experiments, including, APS, HCl (37%), ethyl alcohol, and the desiccant phosphorous pentoxide (P_2O_5) were all received from Merck (Turkey) and used without purification.

B. METHODS

B. 1. Fabrication of POT/Halloysite Clay Composite

0.30±0.0005 g weighed-halloysite was taken to a 50 mL 3-necked round bottom flask and dispersed into 15 mL certain amounts of *o*-toluidine (0.025 M-0.6 M) containing aqueous HCl solution, whose acid concentration was varied between 0.025 M-1.0 M. After gently shaking of the dispersion for a while, the oxidative polymerization was started by the dropwise introduction of 5 mL certain concentration of APS solution (0.0125-0.30 M) prepared in the same HCl solution at 20 ^{o}C. After conduction of the polymerization for a specific time (0.3-6.5 h), the product, POT/halloysite composite, was isolated from the medium through centrifuging at 4000 rpm for 30 min. The composite was then subjected to several washing processes using distilled water and ethyl alcohol, respectively, to separate the residual oxidant and monomer impurities. Finally, it was dried in a vacuum oven at 70°C until reaching a constant weight. The POT content (%) of the composite was determined gravimetrically, considering the initial and final weights of the halloysite samples.

To evidence, the structural change of the composite, pure POT polymer was also prepared similarly to the composite, except for the use of halloysite clay in the procedure.

B. 2. Humidity Sensing Investigation

The humidity sensing performance of the composite in comparison with its components was tested according to the previous works [15, 28]. Accordingly, the samples that were made into pellets were placed into a glass-cell with three necks containing an ice-salt-water mixture. To the one neck of the cell, a thermometer was placed in the same alignment as the sample. Another thermometer was fixed in the ice-bath. When it is started with 0^{o}C, the mixture temperature increased scarcely; namely, the temperatures of the ice-bath and above medium were also measured. The process involves the monitoring of resistivity values of the sample that was changed by the humidity of the medium. When the isolated-system was saturated with the relative humidity, the sample was taken to another chamber containing P_2O_5 as a desiccant. The drying process preceded until the resistivity of the sample remained unchanged. The relative humidity (RH,%) of the medium was calculated according to Equation (1):

$$\text{Relative Humidity (RH, \%)} = [Pw(T_1)/Pw(T_2)] * 100 \quad (1)$$

$P_w(T_1)$ and $P_w(T_2)$ are the saturated vapor pressure of water in the glass cell at T_1 and saturated vapor pressure of water at T_2 temperature in the medium, where the sample is placed, respectively.

B. 3. Characterization

The FTIR spectra were recorded using MATTSON-1000 model FTIR spectrometer after the preparation of pellets from the samples using KBr. The XRD patterns were taken with the Rigaku DMAX IIIC instrument with Cu Kα radiation that is operated at 35 kV and 15 mA (λ = 1.541871 Å). The TGA curves were obtained from the Shimadzu TA50 Thermal Analyzer at a 10 °Cmin^{-1} heating rate under the N_2 atmosphere. The SEM micrographs were monitored by QUANTA 400F Field Emission SEM Instrument, after the application of the Au-Pd coating process.

The electrical conductivity values were calculated by the resistivity measurement of a sample with Thurlby 1503 Digital multimeter, after the preparation of pellets from the samples. The contact angle measurements were performed with an Attension Theta Lite Optical Contact Angle Measurement Instrument using the Sessile Drop method.

III. RESULTS and DISCUSSION

A.1. Effects of Polymerization Time

To determine the polymerization duration for obtaining the highest POT content (%) and conductivity of the composite, first, the polymerization duration was investigated. For that purpose, the polymerization reactions were varied between 0.30 – 6.5 h at 20 °C, and the results are presented in Figure 1. Accordingly, with the increase of the polymerization time, as a possible result of an increase in the POT polymer chain that is contributed to the composite, the POT content (%), as well as the conductivity of the composite, steadily raised to 4 h. The highest POT content (%) and conductivity of the composite took the highest values, including 22.5 (%) and 4.92×10^{-5} $S.cm^{-1}$, respectively. With the further increment of the time, the values showed a decreasing trend. Similar observations were also present in the literature reporting the polyaniline yield and conductivity decrease with increasing polymerization time from 8h to 12 h [29]. Rao et al. correlated the decrease in the conductivity of polyaniline with increasing polymerization time by the further oxidation of polyaniline, from the conducting emeraldine form to the nonconducting pernigraniline form [30]. The reason underlying the decrease in the polyaniline yield (%) was also explained by the excessive oxidation of polyaniline through the breaking of its polymer chain [31]. Consequently, further experiments were conducted for 4h, at which the highest values were provided.

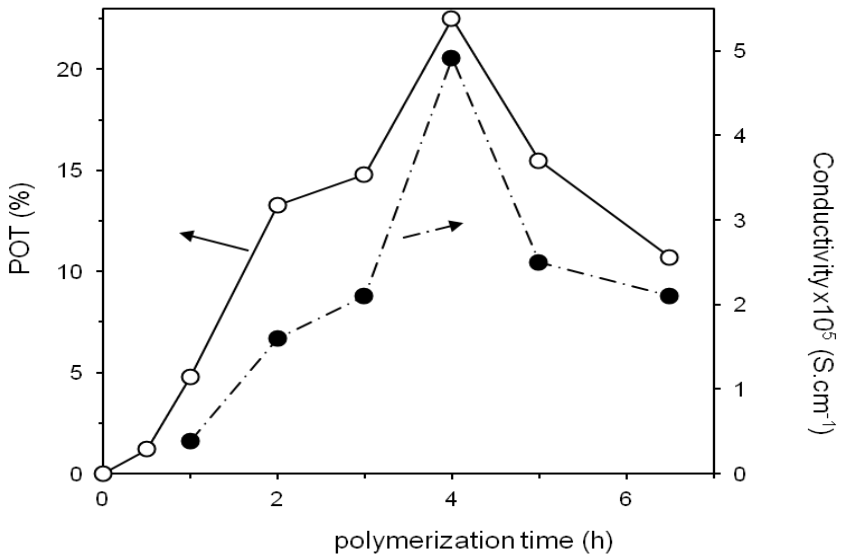

Figure 1. *Changes in POT (%) content and conductivity of POT/halloysite composite with the polymerization time ([APS]: 0.05 M, [o-toluidine]: 0.20 M, medium: 0.40 M HCl)*

A.2. Effects of *o*-toluidine and APS Concentrations

The changes in POT content (%) and conductivity of the POT/halloysite composites were monitored by changing *o*-toluidine and APS concentrations and keeping the other conditions constant, e.g polymerization time as 4h and polymerization medium as 0.40 M HCl. The results are provided in Figure 2. When the results of *o*-toluidine concentration are examined (Figure 2A), the POT content values showed an increasing trend up to the 0.2 M *o*-toluidine concentration and took the highest value as 23.1 % at this point. With the further increment of the concentration, the POT content (%) of the composite slightly decreased and stayed around 20 % (17.5 % at 0.4 M and 20.4 % at 0.6 M). The electrical conductivity values also followed a similar tendency to those of POT contents with a sharper way, including a progressive increase up to 0.2 M and then a decrease over 0.2 M. The increasing of POT content (%) and conductivity of the composite with *o*-toluidine concentration can be explained by the contribution of more amounts of POT chains, and thus, thickening of conductive POT coating on the

clay layers. The possible explanation for the decrease in the POT contents of the composite over a certain monomer concentration may have related to the increase in the viscosity of the polymerization medium [32]. This is generated from the presence of more amounts of the unreacted monomer concerning the amounts of oxidants required for the polymerization. Therefore, the amount of POT polymer that is contributed to the clay layers may have taken lower values compared to that of 0.2 M *o*-toluidine. Since a satisfactory conductive layer formation was not provided at the higher concentrations, the conductivity values also took relatively low values with a similar manner of POT contents of the composite. Consequently, further experiments were continued using 0.2 M *o*-toluidine concentration.

When the results of APS concentration are viewed (Figure 2B), it can be seen that the POT(%) contents of the composite increased with a relatively higher slope up to the APS concentration of 0.1 M, then continued increasing with a lower slope and reached saturation. With the gradual increment of oxidant molecules in the reaction medium, the possibility of the formation of more numbers of oxidized-oligomer derivatives may increase. The combination of these oligo chains may result in the formation of longer polymer chains, an increase in the POT yield, and thus, POT content (%) of the composite that is coated on the clay layers. When the APS concentration reaches a point that is far higher than the *o*-toluidine concentration, the formation of polymer chains with an over-oxidization may have occurred, and this would also increase the POT contents (%) with the lower conductivity values, as the over-oxidated pernigraniline form of polyaniline.

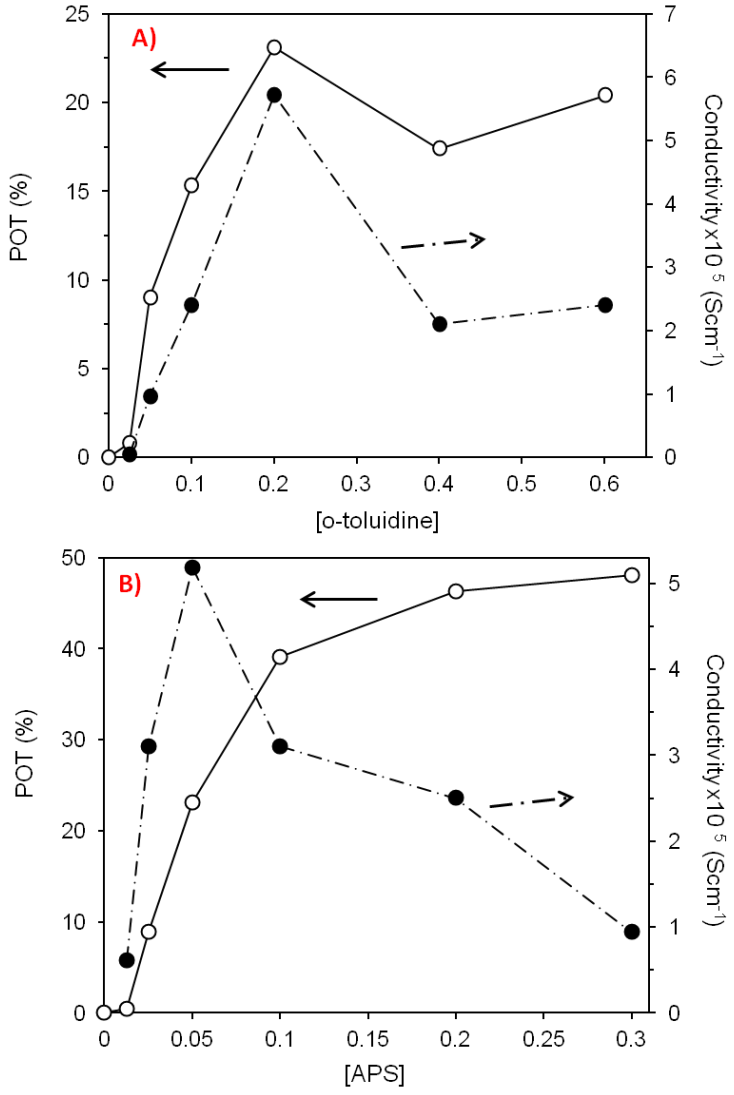

Figure 2. *Changes in POT (%) content and conductivity of POT/halloysite composite with the concentrations change of o-toluidine and APS (polymerization time: 4 h, medium: 0.40 M HCl)*

A.3. Effect of HCl Concentration

The effect of HCl concentration used as the polymerization medium was monitored by running the polymerization reactions at the predetermined APS and *o*-toluidine concentrations for 4h with the changing HCl concentrations between 0.025-0.06 M, and the results are supplied in Figure 3.
Before the experiments, to monitor the possible structural changes that might be occurred to the halloysite in the HCl medium, a blank experiment was also performed, including the mixing of 0.3 g of untreated halloysite particles in the 1.0 M HCl solution. This preliminary test showed that the halloysite has lost 6.4 % of its weight in the acidic solution. This observation was attributed to the loss of Al_2O_3 from the halloysite structure [33, 34], as a possible result of leaching of Al ions from the octahedral layers of halloysite with hydrolysis [34]. Thus, the SiO_2/Al_2O_3 ratio of the halloysite was reported to be significantly increased after the acidic treatment of the halloysite [34].

As seen from Figure 3, the POT content (%), as well as conductivity of the composite, linearly increased with the increment of HCl concentration up to moderate concentration values around 0.5 M, and then remarkably dropped and became the lowest value at 1.0 M HCl concentration. With increasing HCl concentration, the protonation of the *o*-toluidine monomer, and ionic interaction of the monomer with the halloysite layers also increase, yielding the formation of highly doped conjugated POT polymer containing sufficient amounts of Cl^- counter ions on the halloysite. The increase in the conductivity of polyanilines with acid concentration was also correlated with the increased crystallinity of polyaniline, which arose from the linear conformation of polyaniline in the crystalline structure [35]. At high HCl concentration values such as 1. 0 M, the POT chains have been excessively protonated, and this may have transformed the linearly oriented-POT chains to the coiled conformation and decreased the crystallinity[2]. This case was explained by the screening effect in the literature [35, 36].

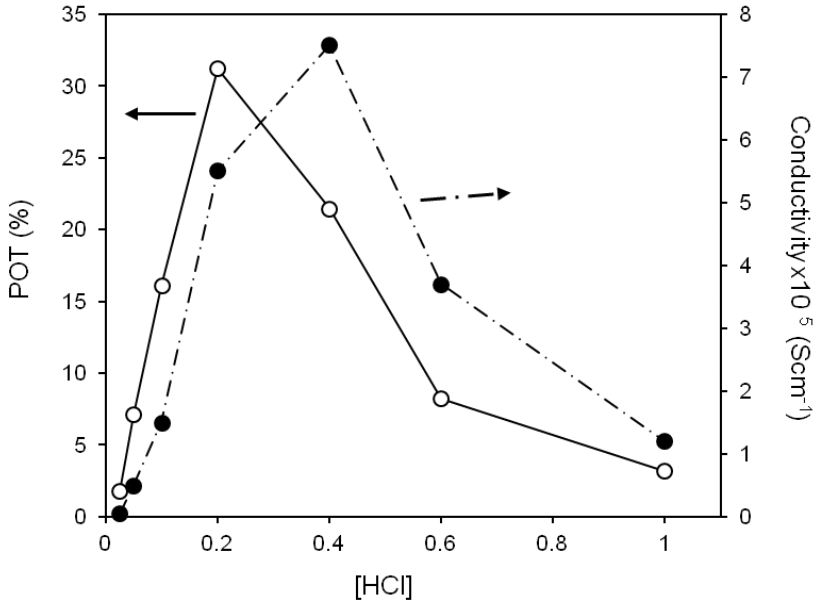

Figure 3. *Changes in POT (%) content and conductivity of POT/halloysite composite with the HCl concentration ([APS]: 0.05 M, [o-toluidine]: 0.2 M polymerization time: 4 h)*

A.4. FTIR Spectra

The FTIR spectra of halloysite, pure POT polymer, and POT/halloysite composite are plotted in Figure 4. As seen from the spectrum of halloysite, the bands at 3697 and 3622 cm^{-1} are attributed to the O-H stretching oh hydroxyl groups present in the inner sırfaces and interlayers, respectively [37]. The band around 3450 and 1633 cm^{-1} are reported to be correlated with the O-H stretching and bending of water molecules, respectively [38]. The rest of the bands, present at the fingerprint region of halloysite, including 1036 cm^{-1}, 913 cm^{-1}, 542 cm^{-1}, and, 472 cm^{-1}, corresponding to the perpendicular Si-O

stretching, Al-OH deformation of the inner hydroxyl groups, Al-O-Si stretching, and Si-O-Si stretching, respectively [20, 39, 40].

In the spectrum of the pure POT polymer, the bands at 1598 and 1487 cm^{-1} correspond to the C=C stretching mode of quinoid rings and C=N antisymmetric stretching modes of benzenoid rings, respectively [41, 42]. The band around 1166 cm^{-1} might have arisen from the stretching vibration of protonated-polyaniline units (quinoid=NH^{+}−benzenoid or benzenoid−NH^{+}−benzenoid), and ultimately, the band observed around 804 cm^{-1} can be assigned to the out of plane deformation of 1,4-disubstituted benzenoid rings of POT [43, 44].

Compared to the spectra of the halloysite and pure POT components, it can be clearly seen that all the determinative bands of the components are present in the spectrum of the composite with the slight shifts, and no new band formation is noticed. This may imply that no chemical interaction was established between the clay and POT in the composite.

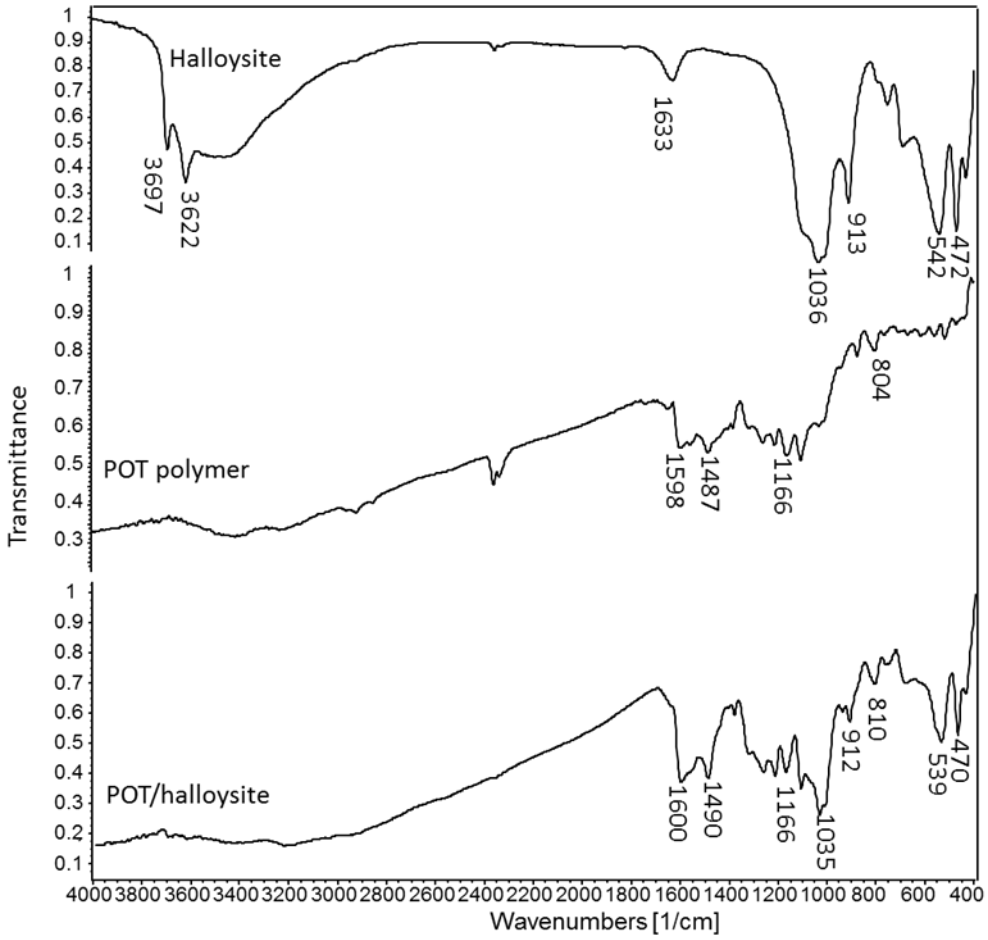

Figure 4. *FTIR spectra of halloysite, pure POT polymer, and POT/halloysite composite.*

A.5. XRD patterns

The XRD patterns of pure halloysite and POT/halloysite composite are provided in Figure 5. As seen from the patterns of the composite and pure halloysite, the diffraction peak arose at 2ɵ°= 12° corresponds to the main reflection plane of (001) halloysite, and the other peaks at 20.1° and 24.7° are identical for the halloysite structure, which is compatible with the JCPDS (29-1487). After the composite fabrication, no significant change was detected in the basal reflection plane of the halloysite, and this may indicate that no significant alteration has occurred in the halloysite structure. Due to the dominancy of halloysite

in the composite and possible superimpositions, POT diffraction bands could not be separately detected in the pattern of the composite.

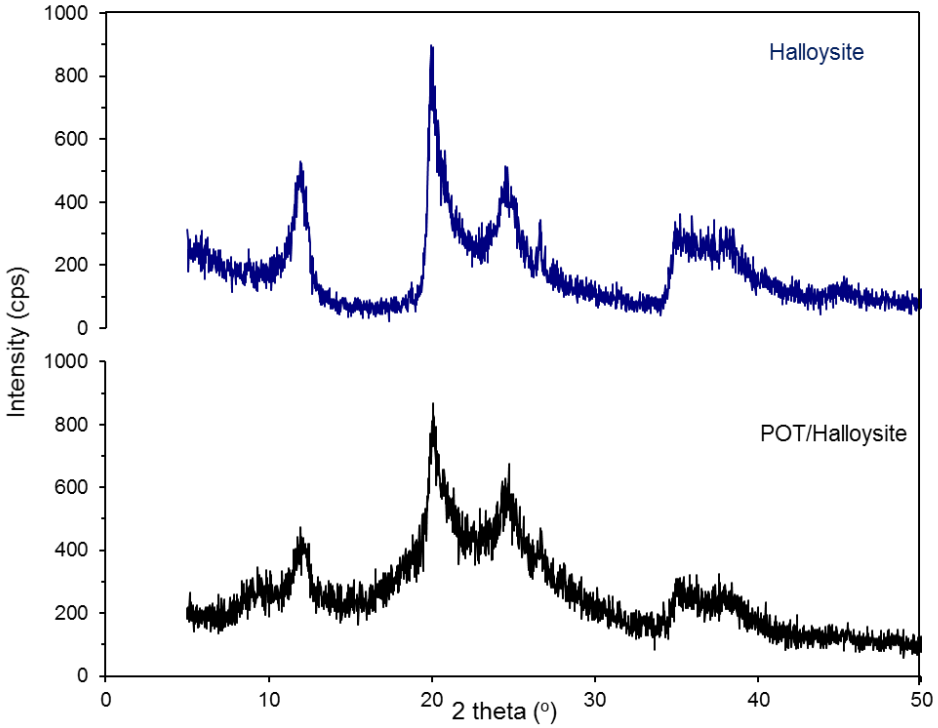

Figure 5. *XRD patterns of halloysite and POT/halloysite composite.*

A.6. TGA Results

The thermal behaviors of the halloysite, pure POT polymer, and POT/halloysite composite containing 20.0 % of POT were monitored by their respective TGA curves, which are given in Figure 6. As gathered from the thermogram of the halloysite, the untreated halloysite shows two-steps of thermal decomposition between 30-100 °C and 350-450 °C (~388 °C), due to the removal of adsorbed water and other possible volatile materials. The total weight loss of halloysite was recorded as 19% between 30-600 °C. The pure POT polymer also shows three-steps of decomposition up to 600 °C (between 0-100 °C, 150-300 °C, and 450-600 °C), as a possible result of removal of moisture, volatile dopant anions contributed to the polymer structure and main chain degradation. The total loss observed in the pure POT polymer's weight was calculated as 65.9 %. When the TGA curve of the composite is viewed, it is seen that the composite demonstrated two-steps of decomposition between 30-200 °C and 350-450 °C (~404 °C), in a similar manner to the untreated halloysite but with relatively higher residual weights. The total residual weight was found as 32 % between 30-600 °C. If the weight loss of halloysite (19 %) up to 600 °C is considered for the composite, it can be seen that the actual weight loss arose from the removal of POT can be practically calculated as 13 %.

In conclusion, if the TGA curve of the POT/halloysite composite is evaluated in terms of its decomposition temperature and residual weight at 600 °C, it can be said that the thermal stability can be improved by the in-situ contribution of POT polymer to the halloysite layers.

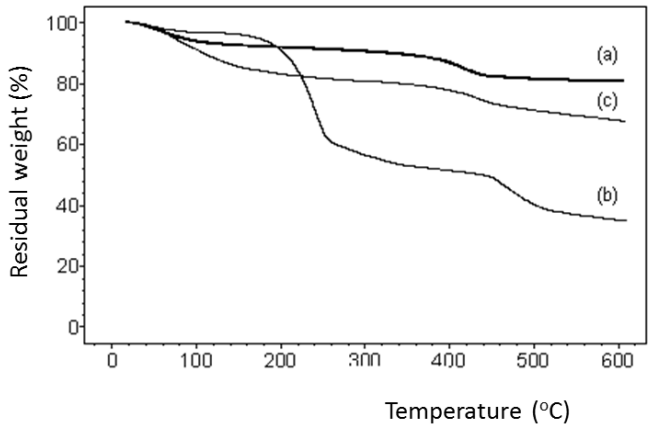

Figure 6. *TGA curves of **a)** halloysite, **b)** pure POT polymer, and **c)** POT/halloysite composite containing 20.0 % of POT.*

A.7. SEM Micrographs

Morphological properties of the untreated halloysite, pure POT polymer, and POT/halloysite composite were identified using the SEM micrographs of the samples that were taken at the different magnifications, and are comparatively presented in Figure 7. As seen from the micrographs of halloysite (Figure 7a and 7d), the halloysite particles comprise of different structures, such as tubes, globules, and layered structures, with different particle sizes ranging from 0.95 μm to 5.5 μm. It is noticed that the halloysite particles can separately be dispersed on the ground without any adhesion/agglomeration signs. It is understood from the micrographs of pure POT polymer that (Figure 7b and 7e) the POT particles have an adherent rock-like structure, and this appearance is more evident from their crumbled fragments. It is thought that the surfaces of the POT polymers get flattened. In the micrographs of POT/halloysite composite, it can be easily seen that the halloysite particles/layers are densely and continuously covered by the POT polymers, giving the impression of no naked/uncovered region is left between the halloysite layers.

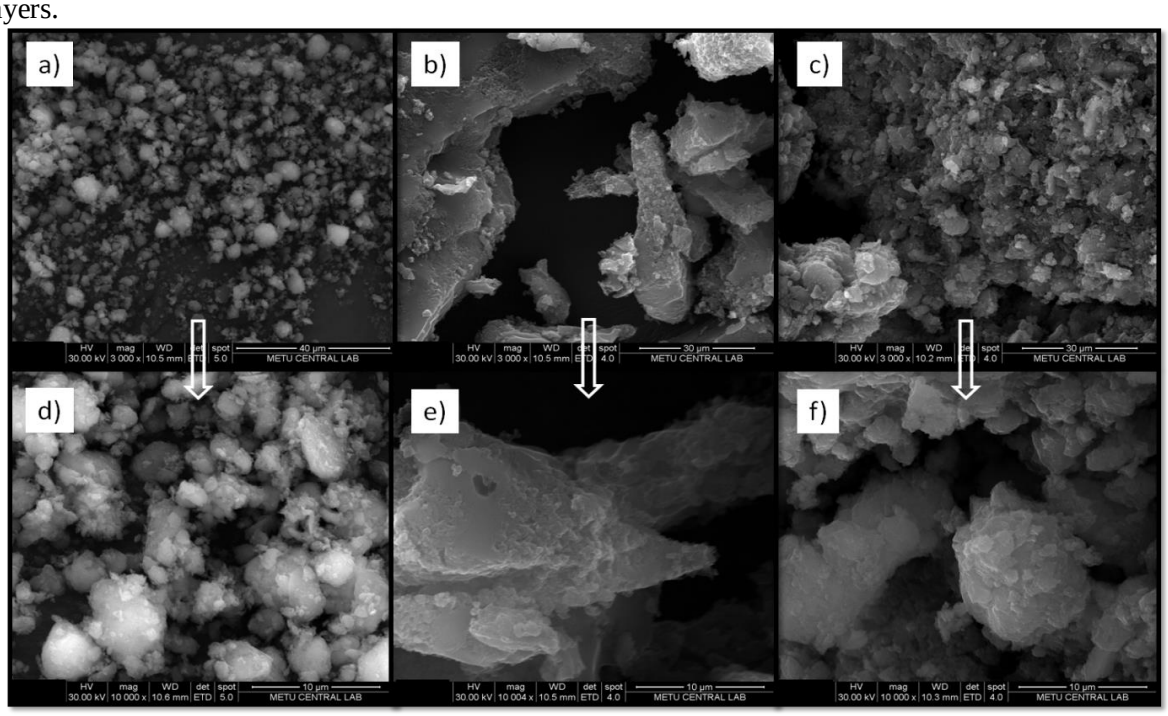

Figure 7. *SEM micrographs of **a), d)** halloysite, **b), e)** pure POT polymer, and **c), f)** POT/halloysite composite.*

A.8. Humidity Sensing Results

The humidity sensing performance of the POT/halloysite composite was evaluated by the resistance changes of the composite with changing the relative humidity (RH) of the medium, and the results are provided in Figure 8, in comparison with a pure POT polymer. After the application of three humidifying-drying processes, the repeatable responses of the resistance were followed. In the first view to the graphs of both samples, the resistance values of pure POT polymer and the composite show a decreasing response with the increment of the RH (%) values from 41% to 94%, and this decrease is more significant for the POT/halloysite composite (Figure 8b). In the first humidifying process, while the POT polymer gave more irregular resistance drops as the response to the RH increase, this trend was more steady and remarkably at the certain RH increase points for the composite, indicating that the POT/halloysite composite has a better performance as a humidity sensor. After the removal of both samples from the first humid medium, and drying on P_2O_5, it was observed that the sensing responses of both of the samples followed relatively regular drops with the RH increase, and this observation became more pronounced at the end of the third humidifying-drying process, which may imply that the samples have reached to an equilibrium.

This observed resistance drop with the increment of RH (%) was explained by the adsorption of water molecules into two steps, including irreversible chemisorption of water molecules onto the hydrophilic surfaces (i.e. -OH groups containing edges of the clay minerals), and reversible physisorption of water (Sears 2008). It is also known that the affinity of a water molecule can also be correlated with the surface properties of the materials, such as hydrophilicity and porosity, namely if the surface of the material has a porous and hydrophilic nature, then the resistance drop would be inevitable. Accordingly, considering the nature of the composite components, it can be concluded that the increase in the hydrophilic nature of the POT polymer by the contribution of halloysite may have improved the electrical response of the material. This statement can also be understood from the net resistance drop values of the samples. For example in the first humidifying process, with the increase of the RH values from 41%-94%, the net resistance change (ΔR) of POT polymer was measured as 705 kΩ, but this change was calculated as 29600 kΩ for the composite. This finding reveals that the presence of halloysite in the composite remarkably improved the responding ability of the POT, thanks to the water adsorption ability of the halloysite.

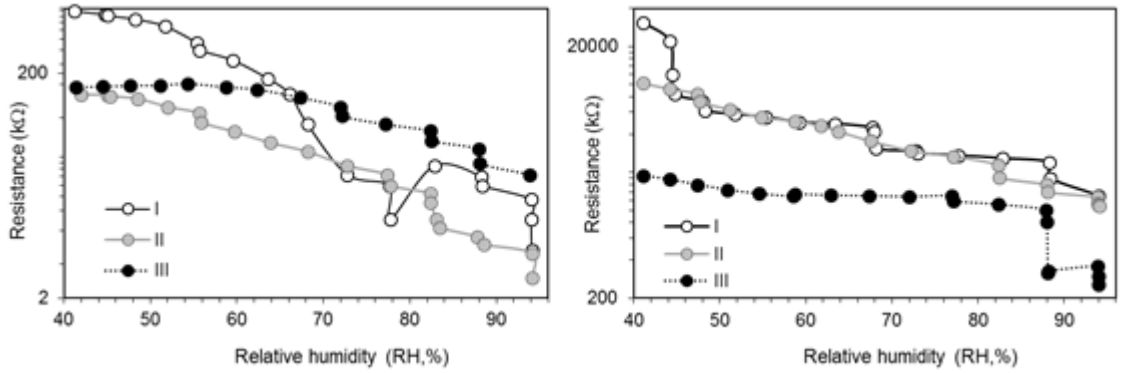

(a) ***(b)***

Figure 8. *Humidity sensing results of* ***a)*** *pure POT polymer and* ***b)*** *POT/halloysite composite for three humidifying processes.*

IV. CONCLUSIONS

With this work, it was demonstrated that one of the most conductive polyaniline derivatives of POT was homogenously and densely incorporated into halloysite clay, for the fabrication of a humidity sensing material. By alteration the various experimental conditions, the POT/halloysite composite with the highest conductivity could be obtained when the polymerization was conducted for 4h using 0.2 M *o*-

toluidine, and 0.05 M APS in 0.4 M aqueous HCl solution. The XRD results confirmed the preserved structure of halloysite even the usage of acidic solutions. SEM micrographs revealed the homogenous deposition of POT onto the halloysite layers. TGA results revealed the improved thermal stability of the composites in comparison to the components. One of the most promoting findings of the study was the humidity sensing responses of the composite, implying that the developed composite may be a successful candidate to be used as the humidity sensor material.

ACKNOWLEDGEMENTS: This work is supported by Ankara University Scientific Project (Project no: 12B4240005).

V. REFERENCES

[1] L. F. B. L. Pontes, J. E. G. de Souza, A. Galembeck, and C. P. de Melo, "Gas sensor based on montmorillonite/polypyrrole composites prepared by in situ polymerization in aqueous medium," *Sensors and Actuators B: Chemical*, vol. 177, pp. 1115-1121, 2013.

[2] N. G. Duran, M. Karakışla, L. Aksu, and M. Saçak, "Conducting polyaniline/kaolinite composite: Synthesis, characterization and temperature sensing properties," *Materials Chemistry and Physics*, vol. 118, no. 1, pp. 93-98, 2009, doi: https://doi.org/10.1016/j.matchemphys.2009.07.009.

[3] F. Boran, S. Çetinkaya, M. Karakışla, and M. Saçak, "Synthesis and characterization of poly(o-toluidine)/kaolinite conductive composites for humidity and temperature sensing," *Pamukkale Üniversitesi Mühendislik Bilimleri Dergisi*, vol. 24, no. 7, pp.1283-1278, 2018.

[4] A. Verma and U. Riaz, "Sonolytically intercalated poly(anisidine-co-toluidine)/bentonite nanocomposites: pH responsive drug release characteristics," *Journal of Drug Delivery Science and Technology*, vol. 48, pp.49-58, 2018, doi: https://doi.org/10.1016/j.jddst.2018.08.024.

[5] H. Zheng, M. Liu, Z. Yan, and J. Chen, "Highly selective and stable glucose biosensor based on incorporation of platinum nanoparticles into polyaniline-montmorillonite hybrid composites," *Microchemical Journal*, vol. 152, pp. 104266, 2020, doi: https://doi.org/10.1016/j.microc.2019.104266.

[6] P. Karthikeyan, S. Sathishkumar, K. Pandian, L. Mitu, and R. Rajavel, "Novel copper doped Halloysite Nano Tube/silver-poly(pyrrole-co-3,4-ethylenedioxythiophene) dual layer coatings on low nickel stainless steel for anti-corrosion applications," *Journal of Science: Advanced Materials and Devices*, vol. 3, no. 1, pp.59-67, 2018, doi: https://doi.org/10.1016/j.jsamd.2017.12.003.

[7] F. J. Anaissi, G. J. F. Demets, R. A. Timm, and H. E. Toma, "Hybrid polyaniline/bentonite–vanadium(V) oxide nanocomposites," *Materials Science and Engineering: A*, vol. 347, no. 1, pp.374-381, 2003, doi: https://doi.org/10.1016/S0921-5093(02)00618-4.

[8] M. Špírková, P. Bober, J. Kotek, and J. Stejskal, "Bi-hybrid coatings: polyaniline-montmorillonite filler in organic-inorganic polymer matrix," *Chemical Papers*, vol. 67, no. 8, pp.1020-1027, 2013, doi: 10.2478/s11696-012-0299-z.

[9] H. Huang, J. Yao, H. Chen, X. Zeng, C. Chen, X. She, and L. Li, "Facile preparation of halloysite/polyaniline nanocomposites via in situ polymerization and layer-by-layer assembly with good supercapacitor performance," *Journal of materials science*, vol. 51, no. 8, pp.4047-4054, 2016.

[10] P. W. Faguy, W. Ma, J. A. Lowe, W.-P. Pan, and T. Brown, "Conducting polymer–clay composites for electrochemical applications," *Journal of Materials Chemistry*, vol. 4, no. 5, pp.771-772, 1994, doi: 10.1039/JM9940400771.

[11] Q. Sheng, D. Zhang, Q. Wu, J. Zheng, and H. Tang, "Electrodeposition of Prussian blue nanoparticles on polyaniline coated halloysite nanotubes for nonenzymatic hydrogen peroxide sensing," *Analytical Methods*, vol. 7, no. 16, pp.6896-6903, 2015, doi: 10.1039/C5AY01329A.

[12] L. Zhang, T. Wang, and P. Liu, "Polyaniline-coated halloysite nanotubes via in-situ chemical polymerization," *Applied Surface Science*, vol. 255, no. 5, pp. 2091-2097, 2008.

[13] X. Sun, Y. Long, P. Wang, J. Sun, and J. Ma, "Preparation of conducting halloysite/polyaniline coaxial tubular nanocomposites in the presence of decorating halloysite as in situ dopant," *Reactive and Functional Polymers*, vol. 72, no. 5, pp.323-328, 2012, doi: https://doi.org/10.1016/j.reactfunctpolym.2012.03.002.

[14] H. Acar, M. Karakışla, and M. Saçak, "Preparation and characterization of conductive polypyrrole/kaolinite composites," *Materials Science in Semiconductor Processing*, vol. 16, no. 3, pp.845-850, 2013, doi: https://doi.org/10.1016/j.mssp.2013.01.009.

[15] M. Günay, M. K. Erdoğan, M. Karakışla, and M. Saçak, "Hydrophobic modification of kaolinite by coating with the conductive polythiophene and investigation of the usability as the environmental-based sensors," *Chemical Papers*, 2020, doi: 10.1007/s11696-020-01268-1.

[16] A. S. Al-Hussaini, "New crystalline poly(aniline-co-benzidine)/bentonite microcomposites: synthesis and characterization," *Polymer Bulletin*, vol. 76, no. 1, pp.323-337, 2019, doi: 10.1007/s00289-018-2386-y.

[17] D. Anaklı and S. Çetinkaya, "Preparation of poly(2-ethyl aniline)/kaolinite composite materials and investigation of their properties," *Current Applied Physics*, vol. 10, no. 2, pp.401-406, 2010, doi: https://doi.org/10.1016/j.cap.2009.06.037.

[18] E. Joussein, S. Petit, J. Churchman, B. Theng, D. Righi, and B. Delvaux, "Halloysite clay minerals - A review," *Clay Minerals*, vol. 40, no. 4, pp.383-426, 2005, doi: 10.1180/0009855054040180.

[19] S. Deng, J. Zhang, L. Ye, and J. Wu, "Toughening epoxies with halloysite nanotubes," *Polymer*, vol. 49, no. 23, pp.5119-5127, 2008, doi: https://doi.org/10.1016/j.polymer.2008.09.027.

[20] E. Tierrablanca, J. Romero-García, P. Roman, and R. Cruz-Silva, "Biomimetic polymerization of aniline using hematin supported on halloysite nanotubes," *Applied Catalysis A: General*, vol. 381, no. 1-2, pp.267-273, 2010.

[21] T. Zhou, C. Li, H. Jin, Y. Lian, and W. Han, "Effective Adsorption/Reduction of Cr(VI) Oxyanion by Halloysite@Polyaniline Hybrid Nanotubes," *ACS Applied Materials & Interfaces*, vol. 9, no. 7, pp.6030-6043, 2017, doi: 10.1021/acsami.6b14079.

[22] F. Hu, J. Xu, S. Zhang, J. Jiang, B. Yan, Y. Gu, M. Jiang, S. Lin, and S. Chen, "Core/shell structured halloysite/polyaniline nanotubes with enhanced electrochromic properties," *Journal of Materials Chemistry C*, vol. 6, no. 21, pp.5707-5715, 2018.

[23] S. Zuo, W. Liu, C. Yao, X. Li, Y. Kong, X. Liu, H. Mao, and Y. Li, "Preparation of polyaniline–polypyrrole binary composite nanotube using halloysite as hard-template and its characterization," *Chemical engineering journal*, vol. 228, pp.1092-1097, 2013.

[24] S. I. A. Razak, N. F. A. Sharif, and I. I. Muhamad, "Polyaniline-coated halloysite nanotubes: effect of para-hydroxybenzene sulfonic acid doping," *Composite Interfaces*, vol. 21, no. 8, pp.715-722, 2014, doi: 10.1080/15685543.2014.932551.

[25] H. Parab, K. Chauhan, J. Ramkumar, R. D. P.S, N. S. Shenoy, and S. D. Kumar, "In-situ synthesised polyaniline - halloysite nanoclay composite sorbent for effective decontamination of nitrate from aqueous streams," *International Journal of Environmental Analytical Chemistry*, pp.1-16, 2020, doi: 10.1080/03067319.2020.1828390.

[26] M. M. Abolghasemi, N. Arsalani, V. Yousefi, M. Arsalani, and M. Piryaei, "Fabrication of polyaniline-coated halloysite nanotubes by in situ chemical polymerization as a solid-phase microextraction coating for the analysis of volatile organic compounds in aqueous solutions," *Journal of Separation Science*, vol. 39, no. 5, pp.956-963, 2016, doi: https://doi.org/10.1002/jssc.201500839.

[27] R. Surya Murali, M. Padaki, T. Matsuura, M. S. Abdullah, and A. F. Ismail, "Polyaniline in situ modified halloysite nanotubes incorporated asymmetric mixed matrix membrane for gas separation," *Separation and Purification Technology*, vol. 132, pp.187-194, 2014, doi: https://doi.org/10.1016/j.seppur.2014.05.020.

[28] M. V. Kulkarni, A. K. Viswanath, and P. K. Khanna, "Synthesis and humidity sensing properties of conducting poly(N-methyl aniline) doped with different acids," *Sensors and Actuators B: Chemical*, vol. 115, no. 1, pp.140-149, 2006, doi: https://doi.org/10.1016/j.snb.2005.08.031.

[29] C. Saravanan, S. Palaniappan, and F. Chandezon, "Synthesis of nanoporous conducting polyaniline using ternary surfactant," *Materials Letters*, vol. 62, no. 6, pp.882-885, 2008, doi: https://doi.org/10.1016/j.matlet.2007.07.003.

[30] P. S. Rao, D. N. Sathyanarayana, and S. Palaniappan, "Polymerization of Aniline in an Organic Peroxide System by the Inverted Emulsion Process," *Macromolecules*, vol. 35, no. 13, pp.4988-4996, 2002, doi: 10.1021/ma0114638.

[31] M. A. C. Mazzeu, L. K. Faria, M. R. Baldan, M. C. Rezende, and E. S. Gonçalves, "Influence of reaction time on the structure of polyaniline synthesized on a pre-pilot scale," *Brazilian Journal of Chemical Engineering*, vol. 35, no. 1, pp.123-130, 2018.

[32] R. Gangopadhyay, A. De, and G. Ghosh, "Polyaniline–poly(vinyl alcohol) conducting composite: material with easy processability and novel application potential," *Synthetic Metals*, vol. 123, no. 1, pp.21-31, 2001, doi: https://doi.org/10.1016/S0379-6779(00)00573-7.

[33] V. M. Abbasov, H. C. Ibrahimov, G. S. Mukhtarova, and E. Abdullayev, "Acid treated halloysite clay nanotubes as catalyst supports for fuel production by catalytic hydrocracking of heavy crude oil," *Fuel*, vol. 184, pp.555-558, 2016, doi: https://doi.org/10.1016/j.fuel.2016.07.054.

[34] K. Belkassa, F. Bessaha, K. Marouf-Khelifa, I. Batonneau-Gener, J.-d. Comparot, and A. Khelifa, "Physicochemical and adsorptive properties of a heat-treated and acid-leached Algerian halloysite," *Colloids and Surfaces A: Physicochemical and Engineering Aspects*, vol. 421, pp. 26-33, 2013, doi: https://doi.org/10.1016/j.colsurfa.2012.12.048.

[35] A. G. MacDiarmid and A. J. Epstein, "Secondary doping in polyaniline," *Synthetic Metals*, vol. 69, no. 1, pp.85-92, 1995, doi: https://doi.org/10.1016/0379-6779(94)02374-8.

[36] M. M. Ayad and M. A. Sheneshin, "Effect of acids on in situ polyaniline film formation," *Polymer International*, vol. 53, no. 8, pp. 1180-1184, 2004, doi: 10.1002/pi.1532.

[37] S. S. Zargarian, V. Haddadi-Asl, and H. Hematpour, "Carboxylic acid functionalization of halloysite nanotubes for sustained release of diphenhydramine hydrochloride," *Journal of Nanoparticle Research*, vol. 17, no. 5, pp. 218, 2015, doi: 10.1007/s11051-015-3032-3.

[38] P. Yuan, P. D. Southon, Z. Liu, M. E. Green, J. M. Hook, S. J. Antill, and C. J. Kepert, "Functionalization of halloysite clay nanotubes by grafting with γ-aminopropyltriethoxysilane," *The Journal of Physical Chemistry C*, vol. 112, no. 40, pp.15742-15751, 2008.

[39] Q. He, D. Yang, X. Deng, Q. Wu, R. Li, Y. Zhai, and L. Zhang, "Preparation, characterization and application of N-2-Pyridylsuccinamic acid-functionalized halloysite nanotubes for solid-phase extraction of Pb (II)," *Water Research*, vol. 47, no. 12, pp. 3976-3983, 2013.

[40] P. R. Chang, Y. Xie, D. Wu, and X. Ma, "Amylose wrapped halloysite nanotubes," *Carbohydrate Polymers*, vol. 84, no. 4, pp.1426-1429, 2011, doi: https://doi.org/10.1016/j.carbpol.2011.01.038.

[41] M. Arora, V. Luthra, R. Singh, and S. K. Gupta, "Study of vibrational spectra of polyaniline doped with sulfuric acid and phosphoric acid," *Applied Biochemistry and Biotechnology*, vol. 96, no. 1, pp. 173-181, 2001, doi: 10.1385/ABAB:96:1-3:173.

[42] M. Trchová and J. Stejskal, "*Polyaniline: The infrared spectroscopy of conducting polymer nanotubes (IUPAC Technical Report),"* in *Pure and Applied Chemistry*, 2011. pp. 1803.

[43] E. T. Kang, K. G. Neoh, and K. L. Tan, "Polyaniline: A polymer with many interesting intrinsic redox states," *Progress in Polymer Science*, vol. 23, no. 2, pp.277-324, 1998, doi: https://doi.org/10.1016/S0079-6700(97)00030-0.

[44] M. I. Boyer, S. Quillard, E. Rebourt, G. Louarn, J. P. Buisson, A. Monkman, and S. Lefrant, "Vibrational Analysis of Polyaniline: A Model Compound Approach," *The Journal of Physical Chemistry B*, vol. 102, no. 38, pp. 7382-7392, 1998, doi: 10.1021/jp972652o.